5ICEGE
5th International Conference on Earthquake Geotechnical Engineering
January 2011, 10-13 | Santiago, Chile

SEISMIC EFFECTIVE STRESS ANALYSIS: MODELLING AND APPLICATION

Misko CUBRINOVSKI [1]

ABSTRACT

The advanced numerical analysis of liquefaction problems is discussed in this paper. The ability of such analysis to accurately simulate behaviour during earthquakes depends on the ability of the constitutive model to represent real soil behaviour. Key requirements for constitutive models targeting liquefaction problems are discussed, and the use of the state concept approach for modelling cyclic behaviour of soils is described. Seismic analysis of two case studies and physical model tests are used to illustrate the application of the seismic effective stress analysis and to demonstrate both its enormous potential and areas where further improvements are needed.

Keywords: Liquefaction, constitutive modelling, seismic analysis, site response, levees, pile foundations

INTRODUCTION

The seismic effective stress analysis is one of the most advanced numerical analyses used in geotechnical engineering. It allows to simulate accurately complex dynamic behaviour of soils during earthquakes including rapid development of pore water pressures, soil liquefaction, and their effects on foundations/structures. Even though this analysis method was formalized in the 1970s/1980s, it has evolved significantly over the past 20 years, especially in the area of constitutive modelling and its application/verification. Recently, the seismic effective stress analysis has been adopted as a state-of-the-art/practice for evaluation of liquefaction problems including assessment of liquefaction-induced displacements, effects on structures and effectiveness of countermeasures against liquefaction (TFR, 2007; ISO, 2005).

In addition to the improved understanding of the physical phenomena and overall computational capability, over the past couple of decades new design concepts have also emerged. In particular, the performance-based earthquake engineering (PBEE) has provided a general framework for seismic evaluation and design of structures. PBEE specifically requires evaluation of deformations and damage to structures in order to assess their performance in strong earthquakes from a modern society perspective. In this context, the new codes of practice are less prescriptive than the older ones and allow the designer to choose an appropriate method of analysis that would meet these PBEE objectives. The new codes are also more demanding, however, and require more detailed evaluation of the seismic response of earth structures and soil-structure systems including nonlinear behaviour, yielding details, transient and permanent deformations, and damage level. The seismic effective stress analysis is well placed to satisfy these rigorous analysis requirements and is hence anticipated to play even more prominent role in the seismic assessment in future.

[1] Associate Professor, Department of Civil and Natural Resources Engineering, University of Canterbury, Christchurch, New Zealand, e-mail: misko.cubrinovski@canterbury.ac.nz

In spite of the great potential of the seismic effective stress analysis, this analysis approach suffers from some of the well known shortcomings of numerical analysis (Potts, 2003). These are particularly pronounced for the effective stress analysis because it uses very complex numerical tools/procedures to simulate even more complex physical phenomena and behaviour during strong earthquakes. Nevertheless, it is important to recognize that there are two key elements to this analysis: the ability of the constitutive model, and the required rigour in the application of the analysis.

This paper begins by discussing the main analysis steps and procedures in the seismic effective stress analysis. Constitutive modelling as a key factor defining the ability of the analysis to accurately simulate real soil behaviour during earthquakes is then examined in detail. Key desirable attributes for constitutive models targeting liquefaction problems are identified, and the use of the state concept approach for modelling cyclic behaviour of sand is outlined. Simulation of case studies and physical model tests are used to illustrate the application of the effective stress method of analysis and demonstrate both its enormous potential and areas where further improvements are needed.

MAIN ANALYSIS STEPS

The seismic effective stress analysis involves the following main steps:

(1) Definition of the numerical model
(2) Determination of parameters of the constitutive model, and
(3) Dynamic analysis and interpretation of results.

In the first step, the numerical model is defined by selecting appropriate element types, dimensions of the model, mesh (element) size, boundary conditions and initial stress state of the soil. Here, one needs to follow the basic rules of a good numerical analysis and consider the geometry of the structure, stratification of the soil deposit, the objectives of the analysis and anticipated behaviour in order to define a numerical model which will facilitate rather than constrain the analysis.

The last two requirements (boundary/interface conditions and initial stress state of the soil) often receive less attention, even though they potentially could have a pivotal influence on the performance of the constitutive model and numerical analysis. Namely, one of the key advantages of the seismic effective stress analysis (and numerical analysis in general) is that no postulated failure and deformation modes are required, as these are predicted by the analysis itself. In this context, the selection of appropriate boundary conditions along end-boundaries or soil-foundation-structure interfaces is critically important in order to allow development of unconstrained response and deformation/failure modes. Similarly, an initial stress analysis is required to determine gravity-induced stresses in the soil and account for their effects on the stress-strain behaviour and liquefaction resistance of soils.

In the second step, parameters of the constitutive model need to be determined using data from field investigations and results from laboratory tests on soil samples. The types and number of laboratory tests required for the parameters of the constitutive model may vary significantly and are model-dependent. In general, however, all models have the same target, and this is to model as accurately as possible the relevant stress-strain relationships of the soil including the development of the pore water pressure and its effects on the stress-strain behaviour of the soil. Needless to say, the above needs to be done for cyclic loading of irregular amplitudes, which is significantly more challenging than modelling of soil behaviour under monotonic loading. It is important to note that whereas most of the constitutive model parameters

can be directly evaluated from data obtained from laboratory tests and in-situ investigations, there are always some parameters that are determined through a calibration process often referred to as *element test simulations*. This is a process in which best-fit values for some of the model parameters are identified through simulations of soil behaviour observed in laboratory tests that practically sets the constitutive model to operate as a simulation tool for the specific soil considered.

In the final step, an acceleration time history is selected as an input ground motion, which is typically defined as a base excitation for the model. Considering the geometry of the problem and anticipated behaviour, numerical parameters such as computational time increment, integration scheme and numerical damping are also adopted, and the dynamic effective stress analysis is then executed. The analysis is quite demanding on the user in all steps including the final stages of post-processing and interpretation of results since it requires an in-depth understanding of the phenomena considered, constitutive model used and particular features of the numerical procedures adopted in the analysis. Figure 1 summarizes the main steps and procedures involved in a seismic effective stress analysis.

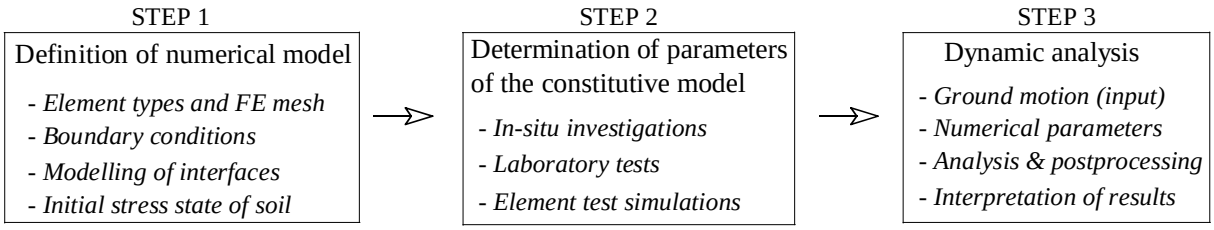

Figure 1. Main steps and procedures in seismic effective stress analysis

The three main steps outlined above should not be considered in isolation, but rather they should be seen as essential components of an integrated process. This realisation is very important and suggests that a good understanding and coherent treatment of all phases and details in the analysis are pivotal for a successful numerical analysis.

Most of the modelling aspects mentioned above will be discussed in more detail and illustrated using simulations of case studies and physical model tests later in this paper. In the following section, we will focus on the constitutive model requirements specific to the seismic effective stress analysis and liquefaction problems.

CONSTITUTIVE MODELLING

The ability of the seismic effective stress analysis to accurately simulate soil behaviour during earthquakes essentially depends on the ability of the constitutive model to represent real soil behaviour. In the case of soil liquefaction this is a very demanding task because the behaviour is very complex involving significant temporal and spatial variation of in-situ conditions/state (changes in the effective stress due to rise of pore water pressures), loads (irregular cyclic stresses) and consequent stress-strain behaviour (highly irregular stress paths including continuous, but also large and abrupt variation in soil stiffness, and significant reduction in strength). Also, post-liquefaction behaviour is often characterized by large ground deformation, permanent displacements, and pore water pressure and voids ratio re-distribution.

While recognizing the complexity of the phenomena considered, the art of modelling is really about selecting and focusing on the most important aspects of the problem considered. Thus a good constitutive model will be tailored to represent the key aspects of soil behaviour for the specific problem at hand, and will provide this ability in an elegant way both from a theoretical viewpoint and practical application. This poses the question: 'What are the most desirable attributes for a constitutive model targeting liquefaction problems?'

Stress-Density Model

To illustrate the desirable features of a constitutive model appropriate for liquefaction analysis, we will examine an elastic-plastic constitutive model for sand, called the Stress-Density Model (Cubrinovski, 1993; Cubrinovski and Ishihara, 1998a; 1998b) which was specifically tailored for analysis of liquefaction problems. The key assumptions of the elastic-plastic formulation of the S-D Model are: (i) continuous yielding or vanishing elastic region; (ii) combined isotropic and kinematic hardening plasticity, (iii) dependence of the plastic strain increment direction on the stress increment direction, or hypoplasticity (a flow rule that accounts for the effects of rotation of principal stresses; Gutierrez et al., 1993), (iv) modified hyperbolic stress-strain relationship, and (v) an energy-based stress-dilatancy relationship. In terms of soil behaviour, this translates into a capability of the model to accurately simulate highly nonlinear stress-strain behaviour both under monotonic loading (from small strains to large strains or steady state of deformation) and irregular cyclic loading. These would be desirable features for any model targeting dynamic problems, in general.

For liquefaction problems, the key requirement is the ability of the model to accurately simulate the development of excess pore water pressures under irregular cyclic loading (earthquake excitation). This ability needs to be demonstrated through a simulation of an experimental liquefaction resistance curve in element test simulations, as discussed below.

The liquefaction resistance curve (LRC) represents the number of cycles (at a given stress ratio $CSR = \tau/\sigma'_{vo}$ or load level) required to cause liquefaction or certain level of strain in the soil, typically 3%, 5% or 7.5% double amplitude strain. The liquefaction resistance curve is commonly derived from a series of liquefaction tests on soil samples in the laboratory in which samples of 'identical' (similar) density are subjected to cyclic shear stresses of uniform amplitude under undrained conditions. Each sample is tested at a different cyclic stress ratio in order to establish the liquefaction resistance across various cyclic stress levels. For example, the open symbols in Figure 2 are results from 6 cyclic torsional shear tests on samples of Toyoura Sand with a relative density of $D_r \approx 60\%$. As indicated in the figure, in Test 3 (T3), 10 cycles were required to cause 3% double-amplitude shear strain when the sample was subjected to a cyclic stress ratio of $CSR = 0.205$. Based on these test data (shown by the open symbols in Figure 2), the experimental liquefaction resistance curve for Toyoura sand with $D_r = 60\%$ is approximated with the dashed line. This liquefaction resistance curve in essence provides an indirect measure for the level of increase in the excess pore water pressure under irregular earthquake excitation.

From a modelling viewpoint, the key objective of the constitutive model is to accurately simulate the experimental liquefaction resistance curve. Typically, this curve is used as a target curve in element test simulations, and one, two or several parameters of the constitutive model are varied in a trial-and-error procedure to identify the best-fit value of the parameter(s) providing the most accurate simulation of the target experimental curve. For the S-D Model, this is achieved by using one of the dilatancy parameters (S_c). For example, in Figure 2, the solid line shows the S-D Model simulated LRC obtained for $S_c = 0.0055$. Note that this line was established through a number of element test simulations of the cyclic behaviour of the soil under various levels of cyclic shear stresses. Figure 3, for example, shows one of

those simulations where the effective stress path and stress-strain curve simulated by the model are presented. In this model simulation, the soil element was subjected to uniform cyclic stress ratio of *CSR* = 0.20 and 11 cycles were required to cause liquefaction and develop 3% double-amplitude shear strain.

The simulation of the liquefaction resistance curve shown in Figure 2 is considered sufficiently accurate for liquefaction analysis. The experimental and analytical LRCs practically coincide for *CSR* values below 0.2 while there is a small discrepancy at higher stress ratios. It is important to achieve a good level of accuracy across wide range of CSRs corresponding to 1-30 cycles, because these are loading levels and

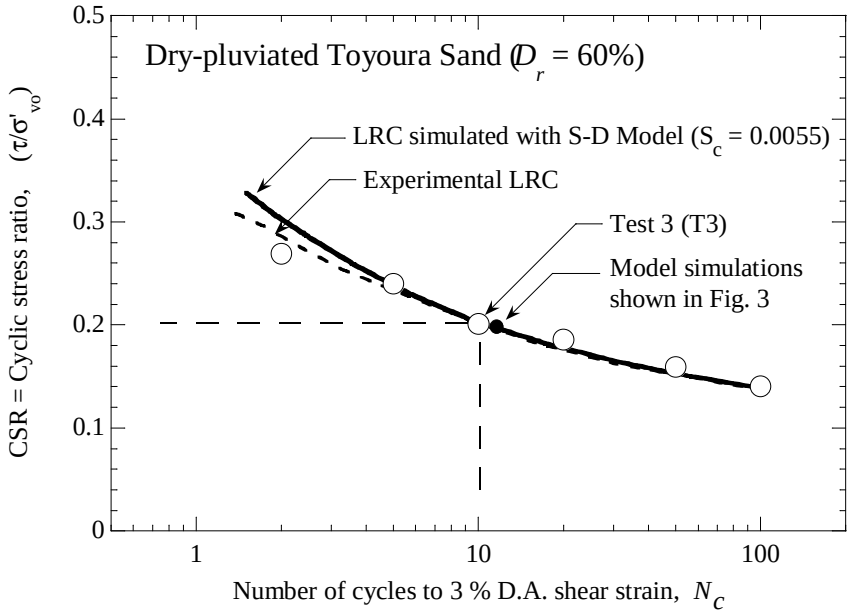

Figure 2. Experimental and simulated liquefaction resistance curves

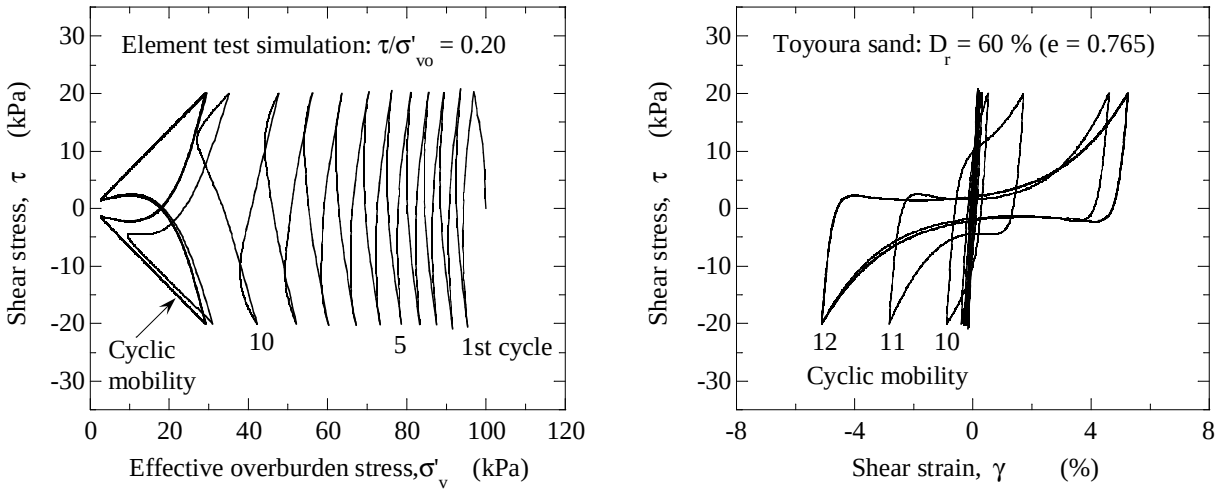

Figure 3. Effective stress path and stress-strain curve obtained in element test simulations with S-D Model for *CSR* = 0.20

cycles relevant for strong ground motions of earthquakes of different magnitudes. Many constitutive models targeting liquefaction analysis fail to accurately simulate the liquefaction resistance curve particularly at low cyclic stress amplitudes. In particular, some models largely underestimate the liquefaction resistance at small stresses, which in turn leads to a completely erroneous pore water pressure build-up in the seismic effective stress analysis. For the example shown in Figure 2, such models will predict liquefaction say for stress ratios of 0.10 even though the experimental results clearly show that the soil could not liquefy if the cyclic stress ratios are below 0.14. Thus, accurate modelling of the threshold *CSR* separating between liquefaction and no-liquefaction is critically important for a good performance of the model across a wide range of earthquake excitations (different acceleration time histories).

Finally, it is also desirable for the constitutive model to have a modelling mechanism that will provide some versatility in the modelling of the cyclic mobility (indicated in Figure 3). In particular, the development of shear strain in subsequent cycles could be very different depending on the density of the soil considered. A constitutive model that provides a controlling mechanism for the development of shear strain during cyclic mobility will predict more accurately both transient and permanent ground deformations associated with soil liquefaction.

In summary, in addition to the desired features for constitutive models appropriate for dynamic analysis, the models targeting liquefaction problems need to:

- Accurately model an experimental liquefaction resistance curve over the relevant range of cyclic shear stresses in the range between N_C = 1-30 cycles
- Accurately model the threshold *CSR* separating between liquefaction and no-liquefaction, and
- Provide a mechanism for strain-development control during cyclic mobility.

State-Concept Approach

Another major feature of the Stress-Density Model is that it utilizes the state concept approach for modelling the combined effects of density and normal stress on the stress-strain behaviour of sand. In this context, there are two key elements to the model.

First, the State Index (I_s) proposed by Ishihara (1993) and Verdugo (1992) is used as a key variable in the model controlling the stress-strain behaviour of sand and in particular the effects of density and normal stress on this behaviour. The inclusion of the state index in the model is very simple and essentially done through a couple of relationships. Figure 4 shows these relationships for Toyoura sand where the initial shear modulus and peak strength of the sand are defined as functions of I_s. Since I_s is a measure for the state of the soil relative to the steady state (similar to the state parameter of Been and Jefferies, 1985), the relationships in essence reflect the fact that sand stiffness and peak strength depend on the density and mean normal stress level. The state concept provides an elegant method for constitutive modelling of the combined effects of density and normal stress on stress-strain behaviour of sand.

Second, the state index is employed in the model as a current variable rather than an initial state parameter (Cubrinovski, 1993; Cubrinovski and Ishihara, 1998a). In other words, the stiffness and peak strength of the sand are dependent on the current value of the state index (i.e. current density and normal stress level, at each loading step). Hence, the stress-strain curve of the soil will change with variation of the current state index (or relative state of the soil). This feature of the model is schematically illustrated in Figure 5 where undrained behaviour under monotonic loading is comparatively shown for a loose sand (with an initial I_s value of ~ 0) and a dense sand (with an initial I_s value of ~ 8). Note that, by definition, I_s takes a value of 1.0 for initial *e-p'* states coinciding with the projection of the steady state line on this

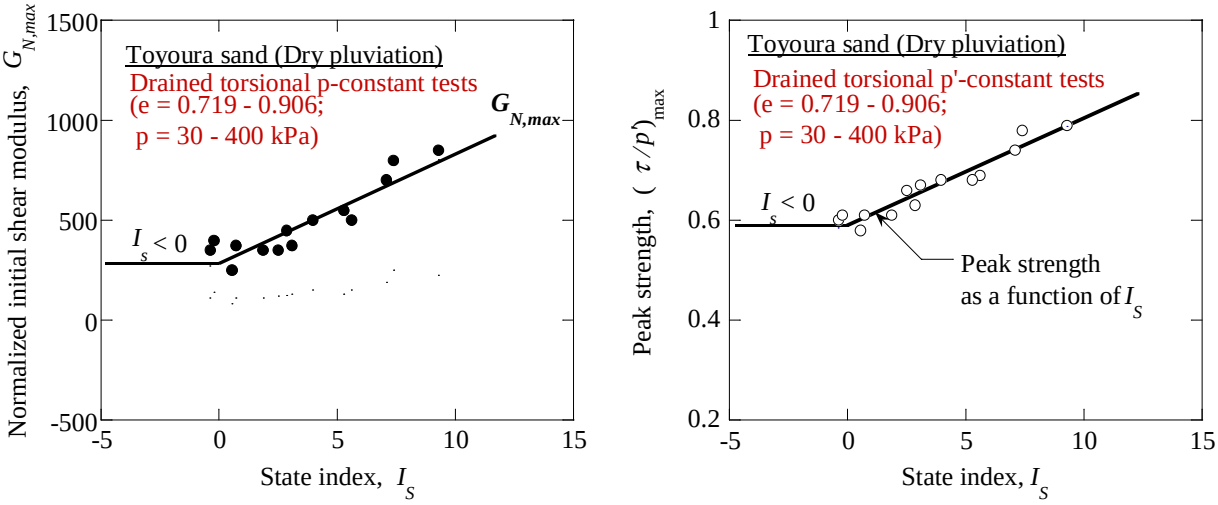

Figure 4. Initial stiffness and peak strength of sand expressed as functions of State Index

plane. Figure 5a shows that for the loose sand I_s remains nearly constant at ~ 0 during the undrained loading, while for the dense sand I_s initially increases reaching a value of 10 at phase transformation, and then decreases with the dilation towards the steady state line and an ultimate value of I_s = 1.0. The *e-p'* paths and variations of I_s for both tests are shown in Figures 5a and 5b, respectively. Figures 5c and 5d show the respective effective stress paths and stress-strain curves, and finally Figures 5e and 5f indicate the variation of the peak strength and change in the stress-strain curve along the undrained paths of these tests. More recently, Gajo and Wood (1999) and Wood (2005) used exactly the same idea in the development of Severn-Trent Sand constitutive model except that they employed the state parameter (Been and Jefferies, 1985) instead of the state index.

Note that the use of the state index as a current state variable permits modelling of strain-softening behaviour even with a conventional hyperbolic model, which is otherwise not possible. In addition this provides an elegant mechanism for modelling of complex post-liquefaction phenomena involving significant change in density/volume such as voids ratio re-distribution.

Modelling Cyclic Behaviour

The state concept approach relies on the use of a state measure (state index or state parameter) for modelling sand behaviour. Both state index and state parameter provide measures for the initial state of the soil (in terms of density and normal stress, e.g. *e-p'* state) relative to the steady state line. Since the steady state of deformation is the ultimate state achieved in monotonic loading tests, the state parameter and state index in effect quantify the state of the soil prior to loading (initial state) in relation to the respective ultimate state (steady/critical state). Clearly, for monotonic loading these two states indicate not only whether the sand will be contractive or dilative, but also the exact amount of dilation or contraction in monotonic loading.

For cyclic loading, however, the above analogy does not apply strictly, because, in this case, the ultimate state upon cyclic loading will not end up at the steady/critical state. Instead, when sheared cyclically under undrained conditions, the soil will develop positive pore water pressure (due to contractive tendency) and eventually liquefy (if loose enough). Hence, the end state will be at the initial void ratio (because of the undrained condition) and p' = 0 (because of liquefaction). Nevertheless, there appears to

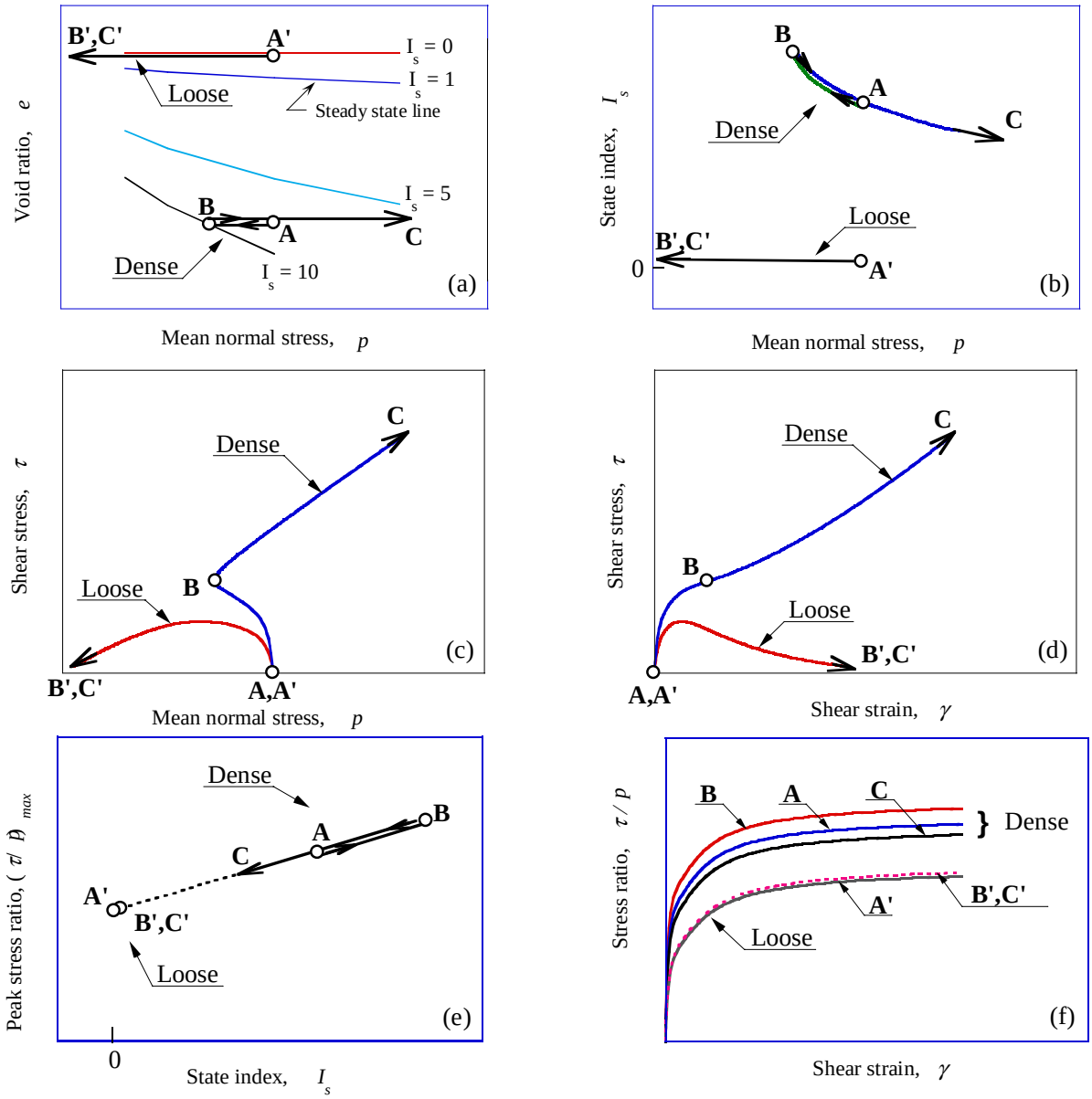

Figure 5. Use of state index as a current variable: schematic illustration of undrained behaviour under monotonic loading (after Cubrinovski and Ishihara, 1998a)

be a close link between the monotonic and cyclic behaviour as far as the tendency for contraction or dilation is concerned. Hence, even though the state concept is not explicitly related to cyclic behaviour, it still provides a very elegant and accurate way of modelling cyclic behaviour. This is illustrated in Figure 6 where simulations of liquefaction resistance curves obtained by the S-D Model are compared to experimental LRCs for five relative densities of Toyoura sand in the range between 40 % and 80 %. Very good accuracy in the simulation of all liquefaction resistance curves is seen despite using a single set of S-D Model parameters. This clearly demonstrates the capacity of the state concept to capture combined effects of density and normal stress on liquefaction resistance and cyclic stress-strain behaviour.

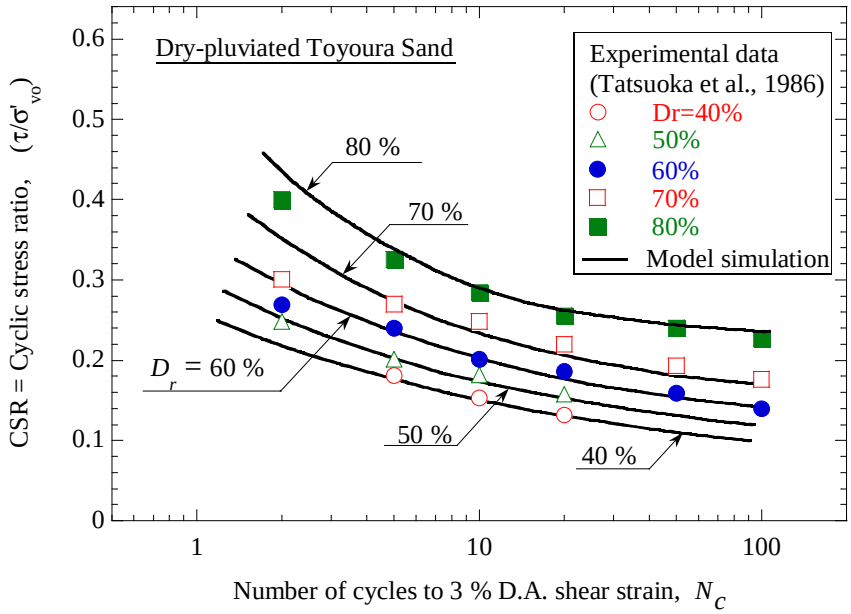

Figure 6. Comparison of experimental and simulated liquefaction resistance curves for various relative densities of Toyoura sand (a single set of model parameters was used in all S-D Model simulations; after Cubrinovski and Ishihara, 1998a)

This also brings to attention another quality of the state-concept approach for sand modelling. Namely, these types of constitutive models are true material models that allow consistent and accurate modelling of any density or initial state of the soil with a single set of constitutive model parameters. An important corollary of this feature is that when determining the parameters of the constitutive model, its overall performance across various densities and effective stress levels is considered, which in turn ensures much better performance of the model in a seismic effective stress analysis. By and large, the state concept approach brings a set of very valuable qualities to constitutive models targeting liquefaction analysis.

In the following sections, we will focus on the application of the seismic effective stress analysis and will re-examine some of the modelling features through analysis of case studies and physical model tests.

FITZGERALD BRIDGE SITE RESPONSE ANALYSIS

The seismic analysis of Fitzgerald Bridge site will be used to illustrate some aspects of application of the seismic effective stress analysis and benefits of such analysis. The Fitzgerald Avenue Bridge is a small-span twin-bridge over the Avon River in Christchurch, New Zealand. The bridge has been identified as an important lifeline for post-disaster emergency services, and hence, it has to remain operational in the event of a strong earthquake. To this goal, a structural retrofit has been considered involving widening of the bridge and strengthening of its pile foundations. A cross section at the mid span of one of the bridges is shown in Figure 7 where both existing piles and new piles are shown. Detailed analysis of the soil-pile-bridge system can be found in Bowen and Cubrinovski (2008) and Cubrinovski and Bradley (2009) while here only free-field site response analyses are presented.

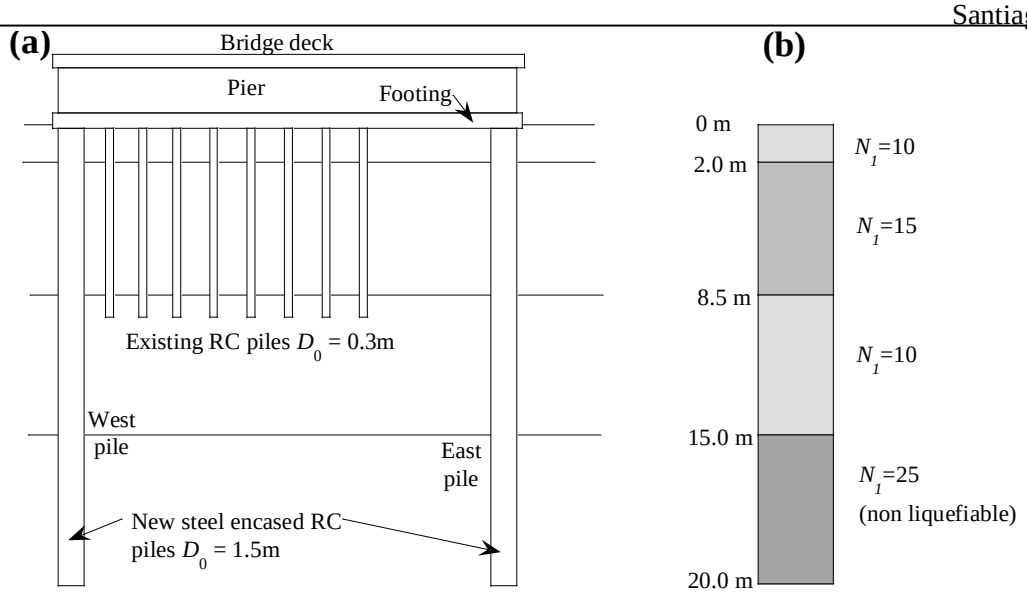

Figure 7. Central pier of Fitzgerald Bridge: (a) cross section; (b) simplified soil profile for seismic effective stress analysis

To optimize the benefits from a seismic effective stress analysis, ideally, high-quality data from field investigations and laboratory tests are needed to feed the numerical analysis and constitutive model. While this would certainly be the preferred method of application of the effective stress analysis, quite often such data is not available. This poses the questions: 'What is the benefit from a seismic effective stress analysis using only conventional geotechnical data as input?', and 'How to calibrate the constitutive model for such analysis?'

Detailed SPT and CPT investigations revealed a large spatial variability of the penetration resistance at the bridge site. From the four abutments for the twin bridges, conventional liquefaction evaluation suggested that only the soils at the north-east abutment were liquefiable. Hence, for a conservative assessment, the profile at the north-east abutment, shown in Figure 8, was adopted for analysis. As shown in the figure, the soil deposit consists of relatively loose to medium dense liquefiable sands with a thickness of about 15 m overlying a dense sand layer. The sand layers have low fines content predominantly in the range between 3 % and 15 %. A comprehensive experimental programme has been carried out on these soils to investigate the effects of fines on the steady state line and liquefaction resistance of reconstituted samples (Cubrinovski and Rees, 2008; Rees, 2010; Cubrinovski et al., 2010a). These detailed studies are beyond the scope of the analysis presented herein, and rather the analysis will be used to demonstrate one approach in modelling the liquefaction resistance based on conventional geotechnical data.

Approximate Modelling of Liquefaction Resistance

For a rigorous determination of parameters of the S-D Model, about 15 to 20 laboratory tests are required including drained and undrained, monotonic and cyclic (liquefaction) tests. In the absence of experimental liquefaction resistance curves for undisturbed samples of Fitzgerald Bridge soils, the liquefaction resistance was determined using the conventional procedure for liquefaction evaluation based on empirical SPT charts (Youd et al., 2001). After an appropriate correction for the fines content and the magnitude of the earthquake (using a magnitude scaling factor representative for M=7.2), these charts

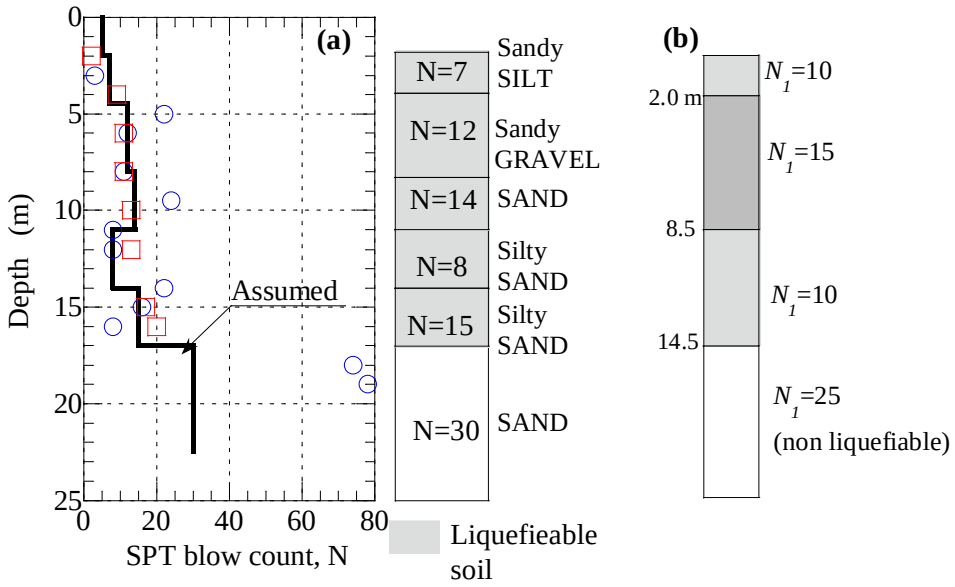

Figure 8. Fitzgerald Bridge site: (a) SPT blow count and soil profile at the north-east abutment; (b) simplified soil profile in terms of normalized SPT blow count

provided the cyclic stress ratios required to cause liquefaction in 15 cycles, for the sand layers with N_1 = 10 and N_1 = 15 respectively. The CSR_{15} values estimated in this way are shown by the solid symbols in Figure 9 in a typical liquefaction resistance curve plot in which *CSR* is plotted against the number of cycles required to cause liquefaction. Using these CSR_{15} values as a target liquefaction resistance in element test simulations, the dilatancy parameters of the model were determined and the liquefaction resistance curves were simulated for the two layers. The two lines shown in Figure 9 represent the simulated liquefaction resistance curves with S-D Model for the soils with N_1 = 10 and N_1 = 15, respectively.

To illustrate better this process, results of element test simulations for the sand with N_1 = 10 are shown in Figure 10 where effective stress paths and stress-strain curves are shown for three different cyclic stress ratios of 0.12, 0.18 and 0.30, respectively. The number of cycles required to cause liquefaction in these simulations and the corresponding stress ratios are indicated with open symbols in Figure 9, depicting the simulated liquefaction resistance. While this choice of material parameters practically eliminates the possibility for a rigorous quantification of the seismic response of the site, one may argue that the parameters of the model defined as above are at least as consistent and credible as those used in a conventional liquefaction evaluation. Note that empirical charts based on CPT could be also employed in the same fashion as described above.

Site Response Analysis

A soil-column model based on the simplified soil profile shown in Figure 8 was subjected to an earthquake excitation with similar general attributes (magnitude, distance and PGA) to those relevant for the seismic hazard of Christchurch. An acceleration record obtained during the 1995 Kobe earthquake (M=7.2) was scaled to a peak acceleration of 0.4g and used as a base input motion. The adopted input motion is neither representative of the source mechanism nor path effects specific to Canterbury, but rather it was considered a relevant excitation typical for the size of the earthquake event considered in the analysis.

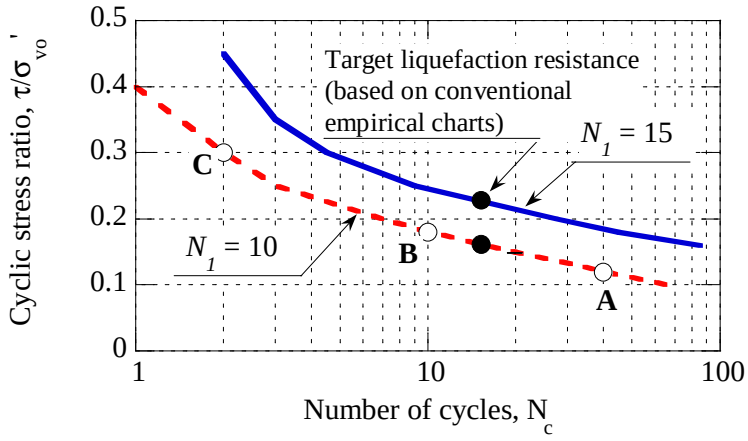

Figure 9. Target liquefaction resistance based on empirical SPT charts and simulated liquefaction resistance curves

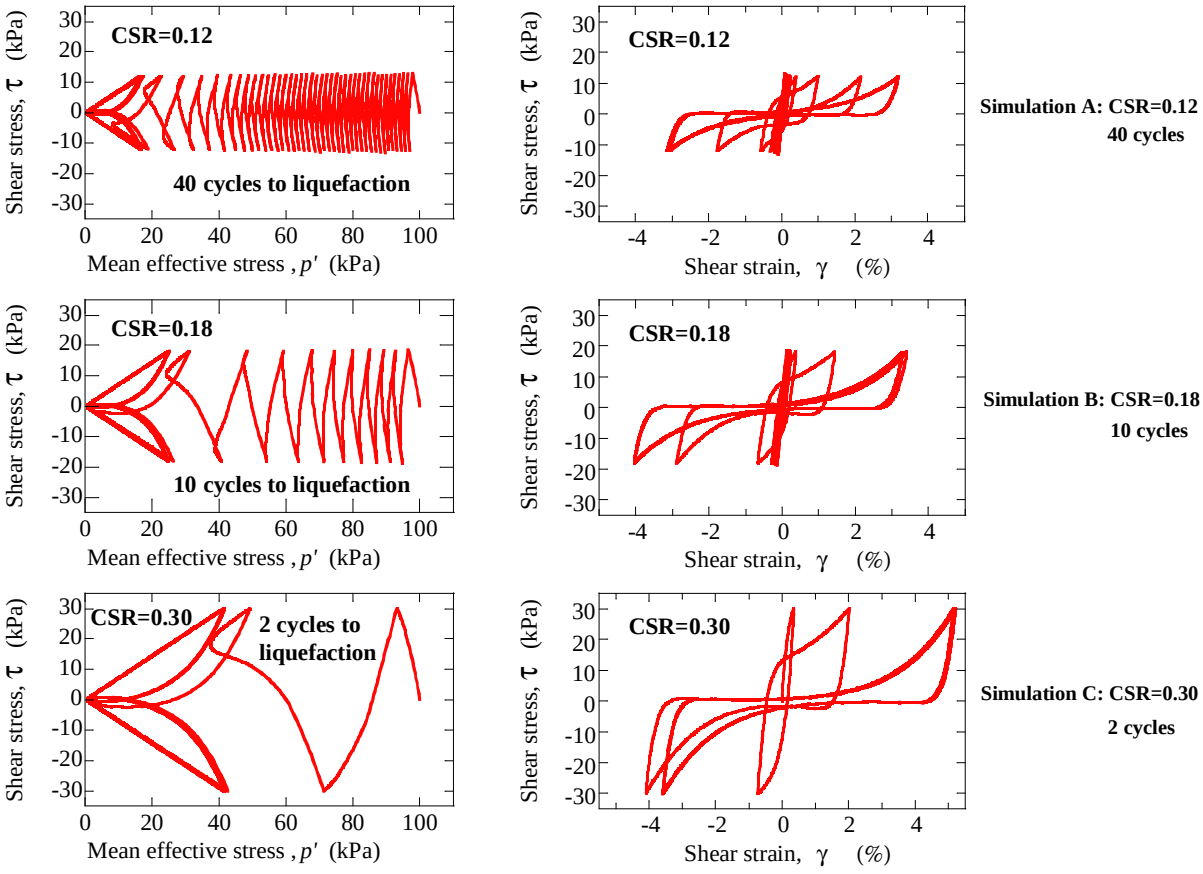

Figure 10. Effective stress paths and stress-strain curves obtained in element tests simulations with S-D Model for soil with N_1 =10

Figure 11a shows time histories of excess pore water pressure computed at two depths corresponding to the layers with N_1 = 10 and N_1 = 15 (z = 13.2 m and 7.0 m respectively). In the weaker layer, the pore water pressure builds-up rapidly in only one or two stress cycles until a complete liquefaction of this layer was reached at approximately 15 seconds. In the denser layer (N_1 = 15), the pore water pressure build up is much slower and affected by the liquefaction in the underlying looser layer. The latter effect is apparent in the reduced rate of pore pressure increase after 15 seconds on the time scale. Clearly, the liquefaction of the loose layer at greater depth produced "base-isolation" effects and curtailed the development of liquefaction in the overlying denser layer. Figure 11b further illustrates spatial and temporal development of excess pore water pressures throughout the depth of the deposit. Note that part of the steady build up of the pore pressure in the upper layer (N_1 = 15) is caused by "progressive liquefaction" or upward flow of water from the underlying liquefied layer. Needless to say, the pore pressure characteristics outlined in Figure 11 will be reflected in the development of transient deformation and permanent displacements of the ground.

Effects of excess pore water pressure are often a key factor in the seismic response of ground and earth structures. Hence, the ability of the effective stress analysis to capture details of pore pressure build-up, development of liquefaction and consequent loss of strength and stiffness in the soil is of great value. The method simulates the most salient features of seismic behaviour of soils including peculiar effects from individual layers and cross interaction amongst them such as "base-isolation effects" or progressive liquefaction due to upward flow of water.

On 4 September 2010, a magnitude M_W7.1 earthquake struck the region of Canterbury, with an epicentre about 40 km west of Christchurch. Widespread liquefaction and lateral spreading occurred in many areas of the city (Cubrinovski et. al., 2010b), though no liquefaction was observed at the Fitzgerald Bridge site and no damage to the bridge was reported. Based on recorded motions in the city area, it is estimated that peak ground accelerations were generally on the order of 0.20-0.25 g. Detailed assessment of the ground response and liquefaction using the effective stress method of analysis is currently in progress.

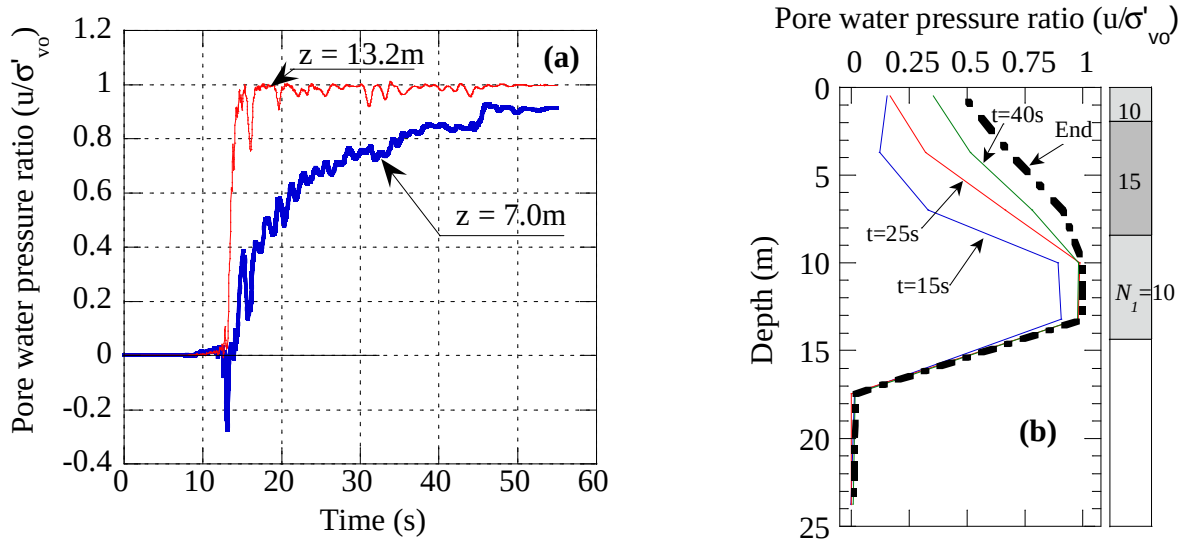

Figure 11. Computed excess pore water pressures in the seismic analysis of Fitzgerald Bridge site: (a) time histories at z = 13.2 m (N_1 = 10) and z = 7.0 m (N_1 = 15); (b) spatial and temporal distribution of excess pore water pressure throughout the depth of the deposit

NARUSE RIVER LEVEES ANALYSIS

The ability of the seismic effective stress analysis to accurately simulate excess pore water pressures and their effects on the response of earth structures and soil-structure systems provides a key role for this analysis in the assessment of effectiveness of countermeasures against liquefaction. A well documented case history on the seismic response of levees (Matsuo et al., 2004; Takahashi and Sugita, 2009) is used to demonstrate this feature of the effective stress analysis.

The 2003 Miyagi-Hokubu Earthquake (M=6.2) caused damage to levees in the epicentral area of Naruse River (Japan). The levees were constructed on loose deposits of old river channels that developed high excess pore water pressures and liquefaction, resulting in large lateral displacements and settlement of the levees.

The subject of the analysis presented herein is a levee section at Nakashimo, near the mouth of Nakase River, about 2 km from the epicentre of the main shock of the earthquake. Prior to the earthquake, about 350 m long section of the levees was improved by installing Sand Compaction Piles (SPC). Four rows of piles with diameter of 700 mm were installed at spacing of 1.7 to 2.2 diameters resulting in a replacement ratio of about 0.1. A cross section of the levees at Nakashimo is shown in Figure 12a where the densified zone is also indicated. The levee is underlain by clayey silts (*A_{Ci} layers*) with over 60 % fines of high plasticity (I_p = 30-67) and sand layers (A_{cs}, A_s) with non-plastic fines of less than 20%.

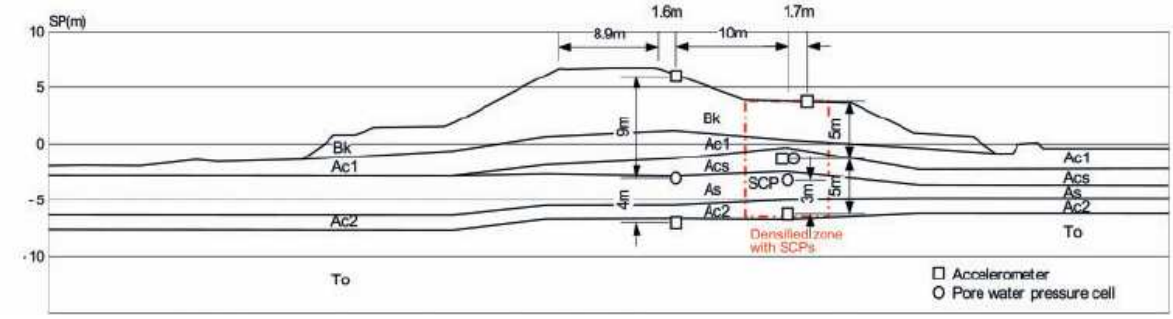

(a) Layout of liquefaction array of accelerometers and pore water pressure transducers

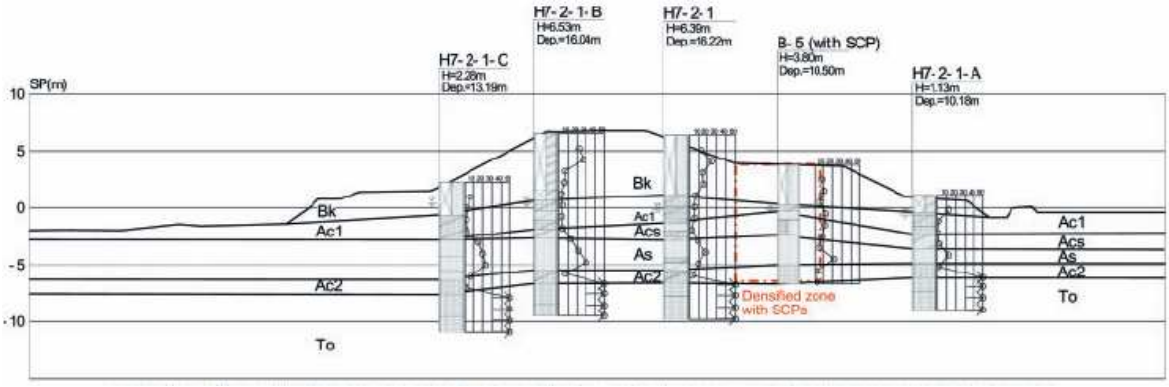

(b) Soil profiles and measured SPT blow count

Figure 12. Cross section of the levees at Nakashimo, right-bank of Naruse River (after Takahashi and Sugita, 2009)

In the central part of the 350 m long SCP-improved section of the levees, a liquefaction array consisting of down-hole accelerometers and pore water pressure transducers was installed in 1998 (Matsuo et al., 2004). Two arrays of accelerometers and pore water pressure cells were installed at the shoulder (unimproved zone) and at the berm (SCP improved zone) respectively. The exact locations of the accelerometers and pore water pressure cells are shown in Figure 12a. Accelerometers were placed at the surface of both improved and unimproved zones, in the middle of the improved zone and at the top of the underlying soft rock. Three pore water pressure transducers were located in the sand layers, one in the unimproved zone and two in the SCP zone. All sensors in the improved zone were installed between the sand compaction piles. Figure 12b shows borehole data and measured SPT blow counts at five locations. In the SCP zone, some (though not significant) increase in the SPT *N*-value is seen for the sand layers. Shear wave velocities of 150 m/s and 650 m/s have been reported for the sandy/silty layers and the underlying soft rock respectively (Takahashi and Sugita, 2009). The soft rock was adopted as a rigid base in the analysis described below.

During the mainshock of the Miyagi-Hokubu earthquake, accelerations and excess pore water pressures (EPWP) were successfully recorded with the liquefaction array. In the unimproved zone, the EPWP ratio (r_u) reached about 0.8 or higher ratios indicating that the untreated sand layers nearly liquefied. The respective ratio in the SCP zone was 0.4 or below. Figure 13 shows acceleration time histories recorded at the top of the base layer (GL-13m) and at the ground surface (GL) in the unimproved zone, near the shoulder of the embankment (Matsuo et al., 2004; Takahashi and Sugita, 2009). Matsuo (2004) reported no apparent damage to the levees in visual inspections and indicated that the settlement of the levee at the liquefaction array site was probably somewhere between few centimetres and 0.2 m.

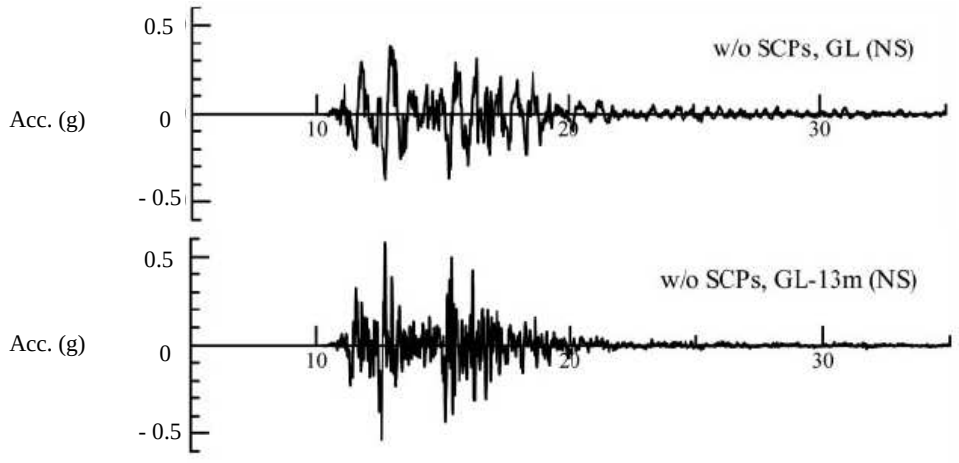

Figure 13. Recorded accelerations in the unimproved zone of the levees at Nakashimo: at the top of the embankment (GL) and at the top of the soft rock layer (GL-13m) (after Takahashi and Sugita, 2009)

Seismic Effective Stress Analysis

An effective stress analysis was conducted using the finite element model shown in Figure 14. The recorded acceleration time history in the soft rock (Figure 13, GL-13m) was used as a base input motion in the analysis.

Results from liquefaction tests on tube samples recovered from the sand layers in unimproved areas indicated cyclic stress ratios of CSR_{20} = 0.19 and 0.23 respectively, for samples from two boreholes: H7-2-1-A and H7-2-1-C in Figure 12 (Matsuo, 2004: Takahashi and Sugita, 2009). Note that these are cyclic stress ratios causing liquefaction in 20 cycles. Based on this information, the liquefaction resistance curve for the sandy soils in the unimproved area was modelled using the S-D model as shown in Figure 15, assuming CSR_{20} = 0.20.

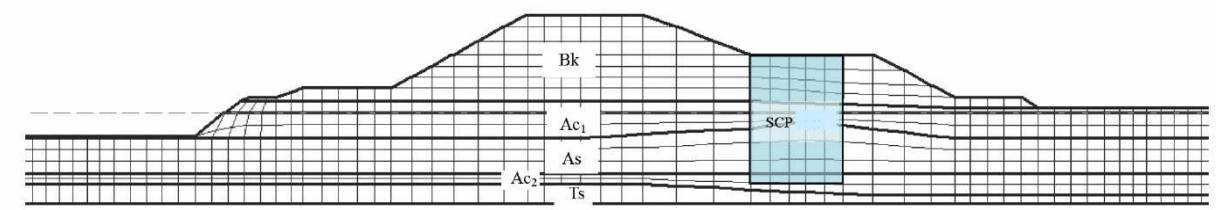

Figure 14. Numerical model used in the effective stress analysis of Naruse River levees

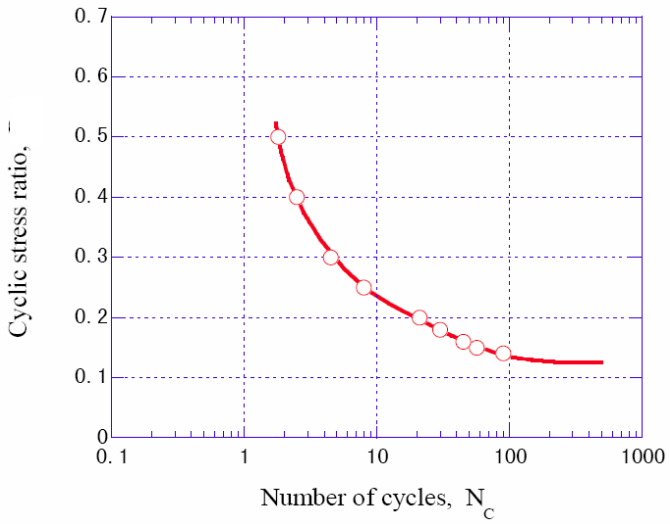

Figure 15. Simulated liquefaction resistance curve for the sand layers within the unimproved zone

The model parameters calibrated for the unimproved zone were used also for the SCP-improved zone, and only the density of the sand was increased based on the replacement ratio to simulate the densification effects due to the installation of SCP. This modelling approach was possible because of the state-concept approach being employed in the constitutive model and because, as descried earlier, the S-D Model as a true material model uses a single set of parameters for modelling a given sand irrespective of its density. The clayey silt layers on the other hand were modelled as nonlinear materials using conventional G-γ relationships and measured shear wave velocities.

Figure 16 shows comparison of recorded and computed excess pore water pressures in the unimproved and SCP zones, respectively. A relatively rapid build-up in the EPWP is seen in the unimproved zone with the excess pore water pressure nearly reaching the initial effective overburden stress or liquefaction

though saturation of the record obscured this detail of the response. In the SCP zone, however, the excess pore pressure build-up was limited to about 40% of the effective overburden stress, thus clearly showing the increase in liquefaction resistance due to sand compaction piles. As shown in Figure 16, the analysis captured these key features of the response and reasonably well predicted the excess pore pressures both in the unimproved and SCP zones. It was found that details of the pore pressure dissipation were affected by the choice of permeability for the clayey silt layers that sandwich the sand layers, however, these details are beyond the scope of this paper.

Figure 17 shows comparisons of recorded and computed acceleration time histories at the top of the unimproved zone of the embankment, where again a good accuracy of the analysis is seen. Similar ground motions and accuracy was also observed for the accelerations at the top of the SCP zone (berm). Again, in good agreement with the observations from visual inspections, the computed lateral displacements and settlement of the embankment were about 0.1 m.

The presented analysis clearly illustrates the potential and accuracy of the seismic effective stress analysis in the assessment of effectiveness of countermeasures against liquefaction and further demonstrates details of its application.

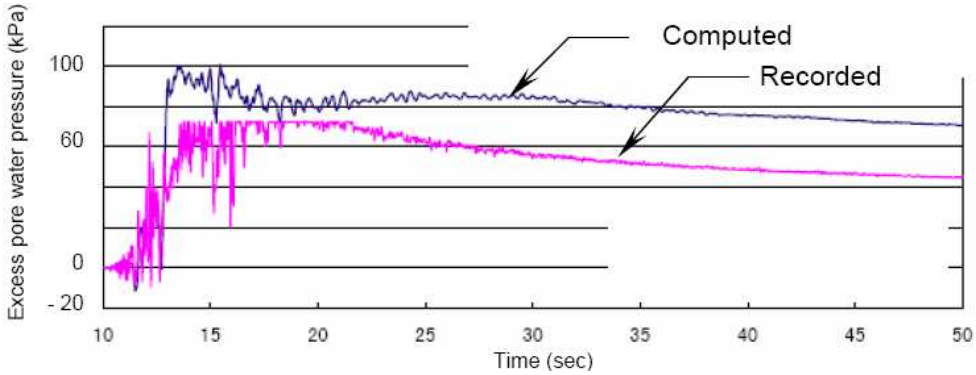

(a) Excess pore water pressures in the unimproved zone (within the shoulder)

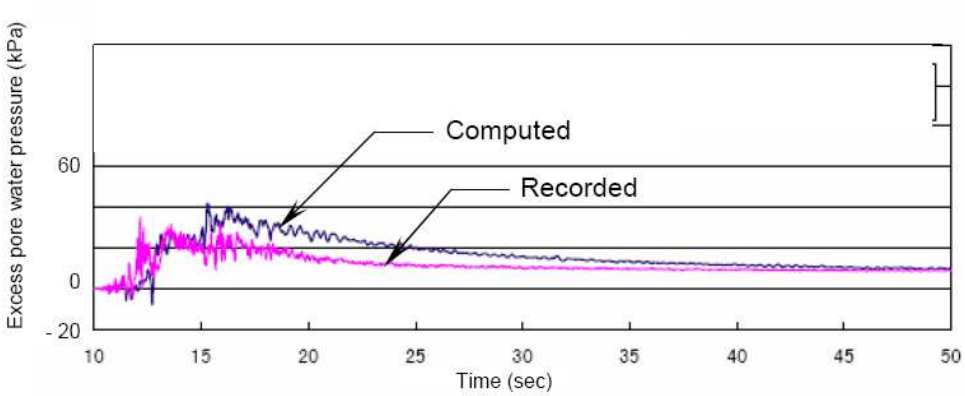

(b) Excess pore water pressures in the SCP zone (within the berm)

Figure 16. Comparison of recorded excess pore water pressures with those computed in the seismic effective stress analysis of Naruse River levees

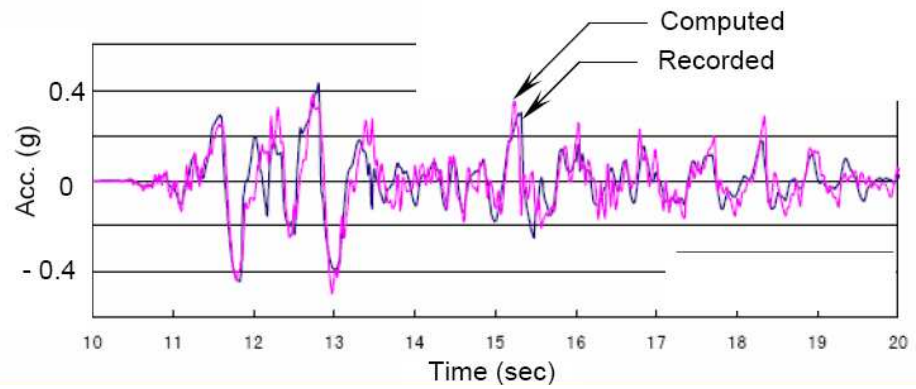

Figure 17. Comparison of recorded excess pore water pressures with those computed in the seismic effective stress analysis of Naruse River levees

3-D SIMULATIONS OF PHYSICAL MODEL TESTS

A comprehensive study on pile foundations in liquefiable soils was carried out in Japan over the period 2002-2007 involving large-scale shake table tests and numerical simulations by advanced methods of analysis (NIED 2006). Within this project, a series of shake-table experiments on piles in liquefying soils undergoing lateral spreading was conducted at the Public Works Research Institute (PWRI), Tsukuba, Japan (Tanimoto et al., 2003). For all experiments, Class-B numerical predictions were made using two different constitutive models and numerical procedures utilizing 3-D effective stress analysis (Cubrinovski et al. 2008; Uzuoka et al. 2008). One of these series of simulations was performed using the S-D Model. Here, some of the results are briefly discussed to highlight both good and bad performances of the seismic effective stress analysis observed in this rigorous verification study.

Various factors were varied in the aforementioned shake table experiments including the amplitude and direction of shaking (transverse, longitudinal and vertical), mass of the superstructure and number and arrangement of piles. A typical physical model used in these tests is shown in Figure 18 consisting of a 3x3 pile foundation embedded in a liquefiable sand deposit, located in the vicinity of a sheet pile wall. The model ground consisted of three sand layers: a crust layer of coarse sand (Iwaki sand) overlying loose liquefiable sand (Toyoura sand with relative density of 35 %), and a dense sand layer at the base (Toyoura sand with relative density of 90 %). The model was built in a rigid container, bottom-fixed at the shake table and subjected to a sine-wave excitation. As indicated in Figure 18, for this particular model three tests were conducted under identical conditions except for the mass of the pile cap/superstructure.

Comparison of Experimental Results and Numerical Predictions

The ground response observed in the tests was characterized by a sudden pore pressure build-up and liquefaction of the loose sand within the first two cycles of shaking. In the course of the subsequent shaking following the initiation of liquefaction, large lateral movement of the sheet pile wall occurred towards the water which was accompanied by ground-flow and spreading of the liquefied backfills.

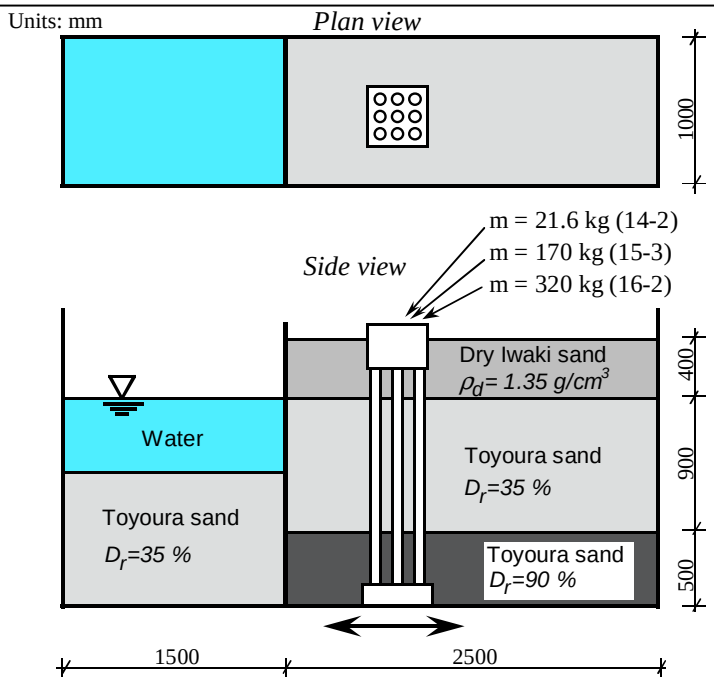

Figure 18. Soil-pile model used in shake table tests

In Test 14-2, for example, the lateral displacement of the top of the sheet pile was approximately 380 mm at the end of the shaking (note that the height of the deposit was 1800 mm). Figure 19 schematically illustrates the deformed configuration of the sheet pile and backfill soils at the end of the shaking. In spite of the large lateral ground movement associated with the spreading of liquefied soils, in this test the peak lateral displacement of the foundation piles was only 12.3 mm and the residual displacement was less than 5 mm. In essence, the pile foundation resisted the ground movement and exhibited *stiff-pile-behaviour*.

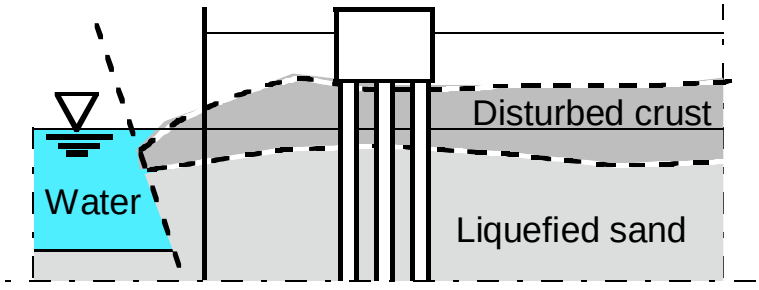

Figure 19. Deformed configuration of backfill soils and sheet pile wall in Test 14-2, after shaking

In general, the numerical predictions were in good agreement with the observations in the experiment capturing the rapid pore pressure build-up, development of liquefaction and consequent ground deformation. In fact, the response of the foundation piles was very well predicted by both analysis methods for all experiments, as indicated in Figure 20, where computed and measured peak horizontal displacements at the pile head are shown for nine different tests. Comparisons of measured and computed peak bending moments for one of the front row piles in three tests are shown in Figure 21, again demonstrating very good agreement between the observed and predicted pile behaviour.

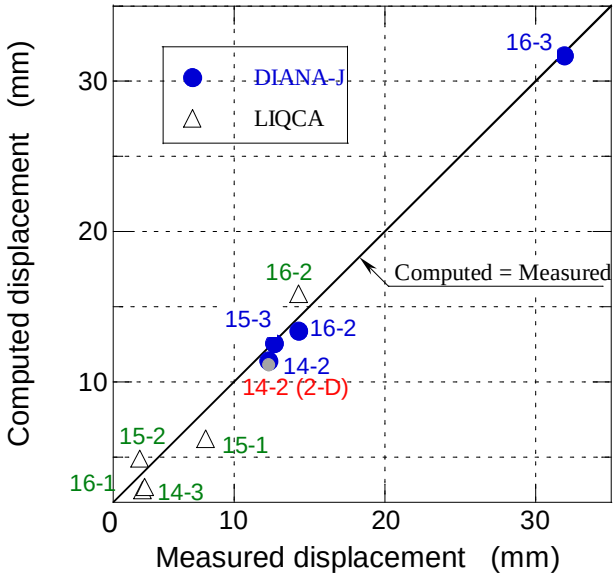

Figure 20. Comparison of computed and measured peak horizontal displacements of pile cap (Class B predictions of 9 experiments)

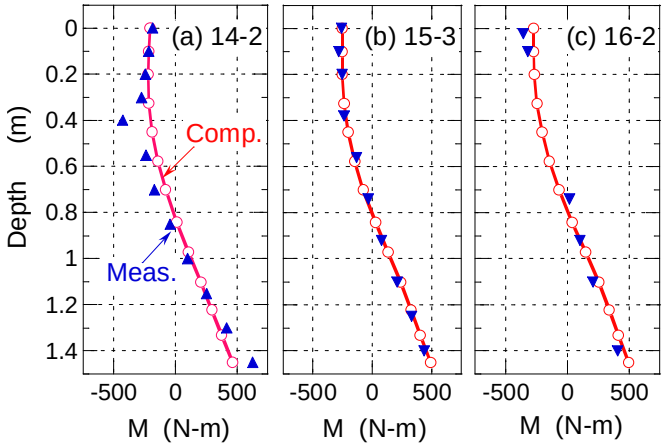

Figure 21. Comparison of computed and measured bending moments of Pile 1 (at the time of peak displacement of pile cap), for experiments 14-2, 15-3 and 16-2

The analyses, however, underestimated the displacement of the sheet pile wall, as summarized in Figure 22. It was found that the prediction of the large lateral movement of the sheet pile wall including instability in the backfills and foundation soils was the most difficult to accurately predict with the advanced seismic analyses. A close scrutiny of the results indicates that the 'average shear strain' in the liquefied soil behind the sheet pile was on the order of 30-40% which is quite challenging to model with conventional soil-pile and soil-wall interfaces located only 600 mm apart (distance between the front-row of piles and sheet pile). In the tests, effects of geometric nonlinearity due to large ground deformation were also significant, as evident in Figure 19, while these were practically ignored in the analyses.

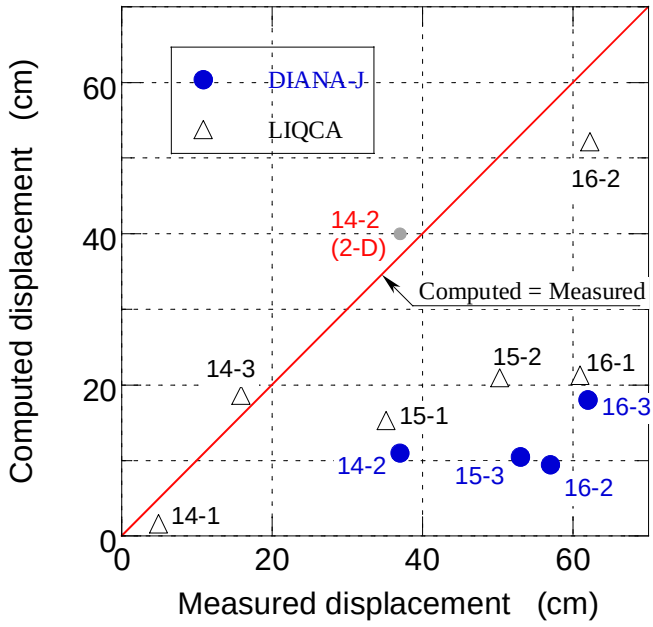

Figure 22. Comparison of computed and measured peak horizontal displacements at the top of the sheet pile (Class B predictions of 9 experiments)

Figure 23 shows a comparison of computed and measured horizontal displacements of the footing/pile cap (pile top) for Test 14-2. Notable is the very good agreement in the first few cycles and subsequent increase in the discrepancy between the computed and measured displacements. The amplitude reduction of footing displacements and elastic rebound of the pile observed in the test is related to the large lateral displacement and settlement of the ground shown in Figure 19. The settlement resulted in a gradual reduction (and eventual loss) of contact between the crust and the back-side of the footing causing reduction in the lateral pressure from the crust on the footing. Since effects of geometric nonlinearity were not considered in the analysis, this deformation mechanism could not be captured in the analysis. The presented results clearly demonstrate the importance of geometric nonlinearity effects in cases involving large ground displacements associated with spreading.

Modelling Issues

Key findings from the benchmark study on the use of seismic effective stress method for analysis of piles in liquefying soils can be summarized as follows.

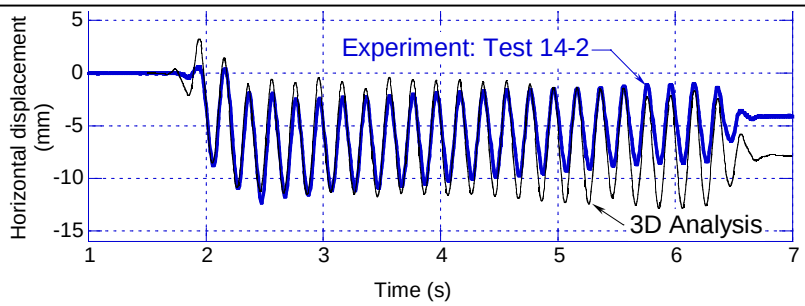

Figure 23. Comparison of computed and measured peak horizontal displacements at the pile top

(i) The ability of the constitutive soil model is critical for the performance of the seismic effective stress analysis. It is essential that the constitutive model provides reasonably good accuracy in predicting the excess pore pressures and stress-strain behaviour of soils in order to allow proper evaluation of the soil-pile interaction effects.

(ii) Details of the numerical procedure, including mesh size, boundary conditions and interface behaviour may significantly influence the predicted response of the soil-pile-structure system. In the abovementioned analyses, initial stresses in the soil were first computed, and specific boundary conditions and soil-pile interfaces were defined in order to allow a deformation pattern associated with lateral spreading to develop. In fact, the limitations of the numerical procedure/model (small-strain formulation ignoring geometric nonlinearity effects) in this regard were found to be the major reason for the deficiencies in the predicted response. Despite the anomalies in the prediction of the sheet pile displacements, however, the peak response of the piles was accurately predicted due to the exhibited stiff-pile-behaviour thus demonstrating the importance of the mode of deformation/failure for the accuracy of the numerical prediction.

(iii) A rigorous implementation of the analysis across all phases (e.g., constitutive model parameters, numerical model and parameters, interpretation of results) is required.

By and large, it was demonstrated through a series of blind predictions that the seismic effective stress analysis could accurately capture the behaviour of piles in liquefying soils undergoing lateral spreading.

CONCLUSIONS

The seismic effective stress analysis permits detailed simulation of dynamic behaviour of soils during earthquakes including rapid development of excess pore water pressures, soil liquefaction and their effects on foundations/structures. It was illustrated through analysis of case studies that in addition to the accurate simulation of spatial and temporal development of pore pressures, the analysis could capture complex effects due to cross-interaction amongst different soil layers, such as “base-isolation” effects due to liquefaction and progressive liquefaction. Accurate simulations of observed pore pressures and accelerations in the levees analysis, and good predictions of the physical model tests on piles in liquefiable soils clearly demonstrate the enormous potential of the analysis. Limitations of both constitutive model and numerical model have to be recognized, including the fact that these limitations are often model-dependent and problem-dependent.

Key to the ability of the seismic effective stress analysis to accurately simulate soil liquefaction is the ability of the constitutive model to represent real soil behaviour. In addition to the desired features for

constitutive models appropriate for dynamic problems, the models targeting liquefaction problems need to accurately simulate the experimental liquefaction resistance curve of the soil. The state concept approach provides an elegant method for modelling cyclic behaviour of sands and a mechanism for an improved performance of the constitutive model in the numerical analysis.

ACKNOWLEDGEMENTS

The author would like to acknowledge the financial support provided by the Earthquake Commission (EQC), New Zealand.

REFERENCES

Been, K. and Jefferies, M. G. (1985). "A state parameter for sands". Geotechnique 35, No. 2, pp. 99-112.

Bowen, H.J. & Cubrinovski, M. (2008). "Effective stress analysis of piles in liquefiable soil: A case study of a bridge foundation". *Bulletin of the NZ Society for Earthquake Engineering*, Vol. 41, No. 4, pp. 247-262.

Cubrinovski, M. (1993). "A constitutive model for sandy soils based on a stress-dependent density parameter". Dr. Eng. thesis, University of Tokyo, Japan.

Cubrinovski, M. and Ishihara, K. (1998a). Modelling of sand behaviour based on state concept. Soils and Foundations, Vol. 38, No. 3, pp. 115-127

Cubrinovski, M. and Ishihara, K. (1998b). "State concept and modified elastoplasticity for sand modelling. Soils and Foundations; Vol. 38, No. 4, pp. 213-225.

Cubrinovski M, Rees SD (2008). "Effects of fines on undrained behaviour of sands". ASCE Geotechnical Special Publication 181: 1-11.

Cubrinovski, M., Uzuoka, R., Sugita, H., Tokimatsu, K., Sato, M., Ishihara, K., Tsukamoto, Y. & Kamata, T. (2008). "Prediction of pile response to lateral spreading by 3-D soil-water coupled dynamic analysis: shaking in the direction of ground flow". *Soil Dynamics and Earthquake Engineering* 28, pp. 421-435.

Cubrinovski, M. and Bradley, B. (2009). "Evaluation of seismic performance of geotechnical structures". Proc. IS-Tokyo2009, Performance-Based Design in Earthquake Geotechnical Engineering, Kokusho, Tsukamoto & Yoshimine (eds) 2009 Taylor & Francis, pp. 121-136.

Cubrinovski, M. Rees, S. and Bowman, E. (2010a). Chapter 6: "Effects of non-plastic fines on liquefaction resistance of sandy soils". Earthquake Engineering in Europe, Springer, pp. 125-144.

Cubrinovski, M., Green, R., Allen, J., Ashford, S., Bowman, E., Bradley, B., Cox, B., Hutchinson, T., Kavazanjian, E., Orense, R., Pender, M., Quigley, M., Wotherspoon, L. (2010b). "Geotechnical reconnaissance of the 2010 Darfield (New Zealand) Earthquake". *Bulletin of the NZ Society for Earthquake Engineering*, Vol. 43, No. 4, (in print).

Gajo, A. and Wood DM. (1999). A kinematic hardening constitutive model for sands; the multi axial formulation". Int. Journal for Numerical and Analytical Methods in Geomechanics, 23, pp. 925-965.

Gutierrez, M., Ishihara, K. and Towhata, I. (1993). "Model for the deformation of sand during rotation of principal stress directions". Soils and Foundations, Vol. 33, No. 3, pp. 105-117.

Ishihara K. (1993). "Liquefaction and flow failure during earthquakes". 33-rd Rankine lecture, Geotechnique 43, No. 3, pp. 351-415.

ISO (2005). "Bases for design of structures – seismic actions for designing geotechnical works". ISO TC 98/SC 3/WG10.

Matsuo, O. (2004). Private communication.

Matsuo, O., Kusakabe, T. Uehara, H., Sekizawa, S. and Sato, S. (2004). Acceleration and pore water pressure responses of SCP-improved levee during the 2003 Miyagiken-Hokubu Earthquake". Proc. 59th Annual Conference of JSCE, 1-775, 1547-1548 (in Japanese).

Potts, D. M. (2003). "Numerical analysis: a virtual dream or practical reality". Rankine Lecture, Geotechnique, Vol. 53, No. 6, pp. 535 – 573.

Rees SD (2010). "Effects of fines on the undrained behaviour of Christchurch sandy soils". PhD Thesis, University of Canterbury, New Zealand.

Takahashi, A. and Sugita, H. (2009). "Behaviour of SCP-improved levee during 2003 Miyagiken-Hokubu Earthquake". Proc. IS-Tokyo2009, Earthquake Geotechnical Case Histories for Performance-Based Design, Kokusho, (ed) 2009 Taylor & Francis, pp. 177-184.

Tanimoto, S., Tamura, K. and Okamura M. (2003). "Shaking table tests on earth pressures on a pile group due to liquefaction-induced ground flow". Journal of Earthquake Engineering, JSCE, 27: Paper No. 339 (in Japanese).

Tatsuoka, F., Ochi, K., Fujii, S. and Okamoto, M. (1986). "Cyclic triaxial and torsional strength of sands for different preparation methods". Soils and Foundations, Vol. 26, No. 3, pp. 23-41.

Task Force Report (2007). "Geotechnical Design Guidelines for Buildings on Liquefiable Sites in Accordance with NBC 2005 for Greater Vancouver Region.

Uzuoka, R., Cubrinovski, M., Sugita, H., Sato, M., Tokimatsu, K., Sento, N., Kazama, M., Zhang, F., Yashima, A. & Oka, F. (2008). "Prediction of pile response to lateral spreading by 3-D soil-water coupled dynamic analysis: shaking perpendicular to ground flow". *Soil Dynamics and Earthquake Engineering* 28, pp. 436-452.

Verdugo, R. (1992). "Characterization of sandy soil behaviour under large deformation". Dr. Eng. thesis, University of Tokyo, Japan.

Youd TL, Idriss IM (2001). "Liquefaction resistance of soils: summary report from the 1996 NCEER and 1998 NCEER/NSF Workshops on evaluation of liquefaction resistance of soils". Journal of Geotechnical and Geoenvironmental Engineering, Vol. 127, No.4, pp. 297-313.

Wood, DM. (2005). "The magic of sand". Canadian Geotechnical Journal, Vol. 44, No. 11, pp. 1329-1350.